# Compound Heat Transfer Enhancement in Dimpled and Sinusoidal Metal Solar Wall Ducts Fitted with Wired Inserts

| Dr. Mohammed H. Mahmoud | Dr. Fouad A. Saleh | Abeer H. Faleh |
|---|---|---|
| Asst. Professor | Asst. Professor | Mech. Eng. Dept. |
| Mech. Eng. Dept. | Mech. Eng. Dept. | Al-Mustansiriyah Univ. |
| Al-Mustansiriyah Univ. | Al-Mustansiriyah Univ. | Baghdad - Iraq |

**ABSTRACT**

An improved Metal Solar Wall (MSW) with integrated thermal energy storage is presented in this research. The proposed MSW makes use of two, combined, enhanced heat transfer methods. One of the methods is characterized by filling the tested ducts with a commercially available copper Wired Inserts (WI), while the other one uses dimpled or sinusoidal shaped duct walls instead of plane walls. Ducts having square or semi-circular cross sectional areas are tested in this work.

A developed numerical model for simulating the transported thermal energy in MSW is solved by finite difference method. The model is described by system of three governing energy equations. An experimental test rig has been built and six new duct configurations have been fabricated and tested. Air is passed through the six ducts with Reynolds numbers from 1825 to 7300.

Six, new, correlations for Nusselt number and friction factor are developed to assess the benefits that are gained from using the WI and the dimpled and sine-wave duct walls. It is found that higher heat transfer rates are achieved using the Dimpled, semi–circular duct with Wired Inserts (DCWI). Also, it is found that Nusselt number and the pressure drop in the DCWI are respectively (44.2% -100%) and (101.27% - 172.8%) greater than those of the flat duct with WI. The improvement in Nusselt number for flat duct with WI is found to be (1.4 – 2) times the values for flat duct with no WI. The results demonstrated that DCWI provides enhancements efficiency value that is higher than those obtained from other types of ducts. The developed MSW ducts have added to local knowledge a better understanding of the compound heat transfer enhancement.

**Keywords :**
 **compound heat transfer, wired  inserts,**
**dimpled duct, sinusoidal duct, Nusselt number.**

**الخلاصة**

(MSW)

(WI)

1825

.7300

WI

.(DCWI)

( %100-%44.2)        DCWI
( %172.8-%101.27)
. WI
( 2 - 1.4 )
.WI                WI

DCWI

Dr. Mohammed H. Mahmoud
Dr. Fouad A. Saleh
Abeer H. Faleh

Compound Heat Transfer Enhancement in Dimpled
and Sinusoidal Metal Solar Wall Ducts Fitted with
Wired Inserts

## 1. Introduction

In Iraq, as well as in many countries in the Middle East, conventional massive external walls of building were designed without consideration to energy consumption. Therefore, research and development of techniques for improvement of thermal performances of existing external walls are of great interest. Metal Solar Wall (MSW) is a dark-colored, multi-duct metal cladding that mounted on the building external walls with a proper air gap between them. The metal ducts can be attached to the existing wall using metal fastening system. The Sun's radiation heats the metal panel, and the heated outside air is drawn through the metal wall ducts by fan mounted at the top of the wall.

The (MSW) system is almost maintenance-free, since there are no liquids or moving parts other than the fan system .So, the cost is minimal ,because the system doesn't require much mechanical equipment, and the metal wall doesn't require to be covered with glass (unlike glazed ,flat- plate solar collectors ). The (MSW) can be designed as an integral part of a new building or it can be added in existing buildings. Actually, the (MSW) can enhance building's appearance even when added after the building is built by covering old, existing walls. Transformation of external walls into solar collectors will protect the building from unwanted summer heat gain, thus reducing the cooling demands and heat losses from building walls. Environmentally, the (MSW) is producing clean renewable energy, thus lowering the need for fossil fuel and reducing the pollution and green-house gases.

The (MSW) is most effective for many types of commercial and industrial buildings with high ceilings, such as; factories, schools, apartments, offices, supermarkets, sport halls, etc. The (MSW) could be used for a wide variety of industrial application such as crop drying, adsorbent beds regeneration in separation processes and  meeting building heating load . In general , vertical walls subjected to a uniform heat flux are used in building components ,passive solar systems, solar collectors and electronic application ( **Beilgen** [2009]).

Using air as a heat transfer media in these systems has some advantages compared with those requiring liquid. Freezing, boiling and corrosion problems are eliminated and the heated air can be used directly without the need for external fluid loop when using air as a working fluid. The major disadvantages of air systems when compared with liquid system arise from low heat transfer coefficient. There are three advantages of employing metal inserts inside ducts. First the porous metal material provides more contact area, so it conducts more heat. Second, the irregularly structure generates an irregular motion of the gas flow, thereby mixing the gas better. Third, as part of solar energy is transmitted through the metal inserts to increase the flowing air temperature, the rest excess energy is stored within the metal material.

Nowadays, a significant number of thermal engineering researchers are seeking for new enhancing heat transfer methods between surfaces and the surrounding gases .Forced convection heat transfer in porous media has many important applications, such as geothermal energy extraction, catalytic and chemical particle beds, petroleum processing, transpiration cooling, solid matrix heat exchangers and packed-bed regenerators.

An experimental investigation has been carried out by **Prasad et al.** [2009] on a packed bed solar air heater using wire mesh as packing material. Data pertaining to heat transfer and friction characteristics were collected for air flow rates ranging from 0.0159 to 0.0347 kg/s-m$^2$ for eight sets of matrices with varying geometrical parameters. It was found that an enhancement of the order of 76.9–89.5% can be obtained. **Aldabbagh et al.** [2011] investigated experimentally the thermal performances of single and double pass solar air heaters with steel wire mesh layers

are used instead of a flat absorber plate. The effects of mass flow rate of air on the outlet temperature and thermal efficiency were studied. The results indicate that the efficiency increases with increasing the mass flow rate. For the same flow rate, the efficiency of the double pass is found to be higher than the single pass by 34-45%.

The use of artificial roughness on a wall surface is an effective technique to enhance heat transfer to fluid flowing in ducts. The application of artificial roughness in the form of dimples on the heat transfer surface may be attractive roughness geometry as it does not require complicated manufacturing process, particularly if the dimple shape is a spherical indentation. Because of this characteristic, dimples do not add extra weight to the absorbing plate. **Hwang et al.[2008]** studied experimentally heat transfer characteristics on various dimple/protrusion patterned walls along with a straight and rectangular test channel. The dimple/protrusion arrays were positioned on top wall only (single-wall) or on both top and bottom walls (double-wall) in each test case. It was found that, for the dimple wall case, flow mixing was higher for the double-wall than the single-wall, which resulted in enhanced heat transfer. An experimental study was carried out by **Saini and Verma[2008]** to investigate the effect of roughness and operating parameters on heat transfer and friction factor in a roughened rectangular duct provided with dimple-shape roughness geometry. The results show that the maximum value of Nusselt number has been found corresponds to relative roughness height (e/D) of 0.0379. **Chang et al.[2010]** studied experimentally heat transfer and pressure drop in hexagonal ducts with smooth and dimpled surfaces .Nu and *f* correlations were individually obtained for each tested hexagonal duct using Re as the controlling parameter. **Durmus et al. [2009]** investigated experimentally the effects of surface geometries of three different type heat exchangers (flat plate, corrugated plate and Asterisk plate) on heat transfer and exergy loss. Results show that the heat

gained from corrugated type is higher than that of the others.

The approach of utilizing simultaneously two different enhancement devices to gain better results compared to that by a single device is known as compound heat transfer enhancement (**Thianpong et al.[2009]**). **Pramanik and Saha [2006]** investigated the heat transfer and friction loss for flow of viscous oil through rectangular and square ducts with internal transverse rib turbulators on two opposite surfaces of the ducts and fitted with twisted tapes. The pressure drop and compound heat transfer characteristics of a converging–diverging tube with evenly spaced twisted tapes were considered by **Mengna et al. [2007]**. Their results showed that the heat transfer rates were 0.85 to 1.21 times of those in a plain tube. **Promvonge and Eiamsa [2007]** investigated the heat transfer characteristics in a tube with combined conical-ring turbulator and twisted tape. An experimental study of turbulent flow in a dimpled tube in conjunction with a twisted tape has been performed by **Thianpong et al.[2009]**. The experiments were performed using water as working fluid for Reynolds number in the range of 12000 to 44000.

The advantages of the compound heat transfer enhancement, shown in literature review, motivate us to investigate heat transfer enhancement inside MSW ducts. However, the survey of available published literature reveals a lack of information about the thermal-hydraulic behavior of dimpled or sinusoidal duct walls, together with the WI as compound enhancing device at the same time.  Also, most of the previous investigations related to heat transfer enhancement have been done for flow of high Reynolds number. The range of Reynolds number investigated by them is not suitable for the airflow in solar air heater ducts **Saini and Verma[2008]**.

To the best of the author's knowledge the heat transfer correlations for ducts of dimpled or sinusoidal walls that subjected to heat flux (in conjunction with the WI), has not been

Dr. Mohammed H. Mahmoud
Dr. Fouad A. Saleh
Abeer H. Faleh

Compound Heat Transfer Enhancement in Dimpled
and Sinusoidal Metal Solar Wall Ducts Fitted with
Wired Inserts

investigated. Therefore, the main objectives of this work are to:

1. Investigate the combined effect of Wired Inserts (WI) together with different ducts surface profile (wavy, dimpled and flat) on heat transfer and flow friction .Both square and semi-circular ducts geometries shall be tested.

2. Develop a computational method to predict the thermal behavior of the (MSW) at any time. The method should be applicable for different duct geometries, inserts and surface profiles.

3. Investigate experimentally the developed laboratory scale ducts that are made locally. The duct is subjected to uniform heat flux to simulate the MSW using air as a working fluid.

4. Propose a developed method for evaluation of Nusselt number correlations for each new type of the MSW ducts.

## 2. Numerical Model

The numerical model proposed in this work consists of metal ducting that containing arbitrary shape wired inserts (WI), and is subjected to solar energy. The experimental results of **Dukhan and Chen** [2007] showed that the thermal boundary condition was neither uniform heat flux nor uniform wall temperature; a typical situation in solar collectors. So, the heated wall temperature was averaged and the heat transfer correlations were based on the uniform wall temperature boundary condition (**Dukhan and Chen** [2007] ) .

The metal WI consists of irregularly-shaped flow passages. Convection and conduction heat transfer occurs between the metal ducting, solid WI and the flowing fluid. The geometric complexity and the random orientation of the solid material in the WI make exact solutions of the governing transport equations inside the pores virtually impossible (**Piao et al.** [1994]). Taking a volume element (dv) contained between ( x ) and (x + dx) over a time interval (dt) , three transient governing energy equations can be written for ducts with wire inserts (WI) , as shown in Figure (1 ).
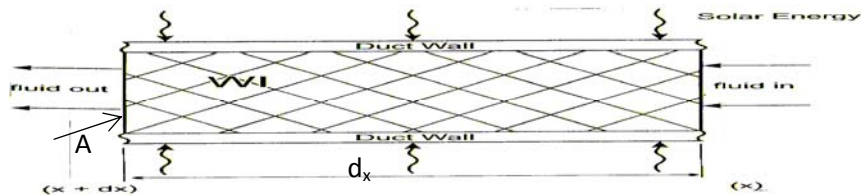


**Figure (1): The control volume of the wired inserts duct.**

The energy balance equation of the flowing fluid inside the control volume is;

*Change of enthalpy of the flowing fluid with respect to time + Change of enthalpy of the flowing fluid with respect to axial position = net conduction heat transfer of the fluid inside the control volume + convection heat transfer between fluid and WI + convection heat transfer between fluid and duct walls*

Therefore, the thermal equation describing the flowing fluid temperature is described by the following partial differential equation ;

$$\rho_a . A . dx . \varepsilon . C_a . \frac{\partial T_a}{\partial t} . dt \ + \ \rho_a . u_a A . C_a . \frac{\partial T_a}{\partial x} . dx . dt \ =$$

$$K_a . A . \frac{\partial^2 T_a}{\partial x^2} . dx . dt \ + \ h . dAc \ .( T_a - T_{WI} ). dt \ + \ h_D . A_{SD} .( T_a - T_D ). dt \ .....( \ 1 )$$

For the wired inserts (WI) within the control volume, the energy balance is ;

*Change of enthalpy of the WI with respect with time = convection heat transfer between fluid and WI*

So, the following partial differential equation describes the transient thermal balance;

$$\rho_{WI}.A.dx.(1-\varepsilon).C_{WI}.\frac{\partial T_{WI}}{\partial t}.dt = h.dA_c.(T_{WI}-T_a).dt \quad .......... \quad ........(2)$$

For the duct walls, the energy balance equation is ;

*Change of enthalpy of the duct walls with respect with time = net conduction heat transfer of the duct walls + convection heat transfer between fluid and inside duct walls + convection heat transfer between ambient and outside duct walls*

Therefore, the transient governing differential equation of the duct walls will be;

$$\rho_D.A_D.dx.C_D.\frac{\partial T_D}{\partial t}.dt = K_D.A_D.\frac{\partial^2 T_D}{\partial x^2}.dx.dt + h_D.A_{SD}.(T_D-T_a).dt + h_{SDo}.A_{SDo}.(T_{Do}-T_\infty).dt .....(3)$$

The coupled set of equations (1), (2), and (3) is approximated as a finite-difference equations to be ;

$$\rho_a.\varepsilon.C_a.[T_a(i,j,t+1)-T_a(i,j,t)/\Delta t] + \rho_a.u_a.C_a.\frac{Ta(i+1,j,t+1)-Ta(i-1,j,t+1)}{2(\Delta x)}$$

$$= K_a.\frac{Ta(i+1,j,t+1)-2.Ta(i,j,t+1)+Ta(i-1,j,t+1)}{(\Delta x)^2} +$$

$$h.A_s.[T_a(i,j,t+1)-T_{WI}(i,j,t+1)] + h_D.A_{DV}.[T_a(i,j,t+1)-T_D(i,t+1)] ........ ..(4)$$

$$\frac{T_{WI}(i,j,t+1)-T_{WI}(i,j,t)}{\Delta t} = [h.As / \rho_{WI}.(1-\varepsilon).C_{WI}].[T_{WI}(i,j,t+1)-$$

$$T_a(i,j,t+1)]........ .........(5)$$

$$\rho_D.C_D.\frac{T_D(i,t+1)-T_D(i,t)}{\Delta t} = K_D.\frac{T_D(i+1,t+1)-2.T_D(i,t+1)+T_D(i-1,t+1)}{(\Delta x)^2}$$

$$+ h_D.A_{DD}.[T_D(i,m,t+1)-T_a(i,t+1)] + h_{Do}.A_{DD}.[T_{Do}(i,t+1)-T\infty(i,t+1)]........ .........(6)$$

where;   $A_{DV}=A_{SD}/A.d_x$ ,   $A_S=dA_c/A.d_x$ ,
and     $A_{DD}=A_{SD}/A_D.d_x$

The initial conditions involve assigning the initial temperatures of WI, air, and duct wall at each node. The formulation of the entrance plane boundary condition is done by assigning the inlet air temperatures. Since no further heat transfer after the air leaves the duct, the exit plane boundary condition is formulated by using backwards difference approximation for $\partial T/\partial x$.

The above equations are solved using a fully implicit scheme. The solution of the set of linear equations is accomplished with a decomposition and back-substitution algorithm for a banded matrix. The grid meshes and time steps sensitivity studies have been performed. The computational runs show that the algorithm was insensitive to spatial increment sizes. The coefficient matrix is updated after each iteration, with air properties and transport coefficients.

## 3. Experimental Setup

Figure (2) presents a schematic diagram of the experimental facility. Tests were carried out using a rig composed of three duct sections, joined together by flanges and screws. As shown in Fig. (2), a pair of ducting geometries were manufactured, one has a square cross-sectional dimensions of (6cm x 6cm) and the other of a semi-circular with diameter of (d=9.82 cm) .These ducts have been manufacturing from copper (CuZn37) (0.5 mm in thickness and 5.812 g/cm³ in density) which have the following chemical

composition (tested at the engineering testing laboratories department in Specialized Institute for Eng. Industries):
37.76%Zn,0.008%Pb,0.026%Sn,0.006%P,0.0005%Mn,0.037%Fe,0.004%Ni,0.001%Si,0.001%Cr, 0.01%Ag, 0.008%As, 0.01%Sb and Bal. cu%

For the purposes of comparison, three ducts have been constructed in the local workshops to have the same hydraulic diameter as shown in Figure (2).

For square duct;  $d_h = 4(a.a)/ (4a)$       (7)

and for semi –circular duct ;

$$d_h = 4( \pi d^2 / 8 ) / [(\pi d / 2) + d]$$       (8)

A honeycomb rectifier installed at the entrance section, followed by three screens, 10 mm apart from one to another ,were employed in order to remove eddies and provide a more uniform velocity profile. However, the entrance duct has a length of 600mm, which is ten times the hydraulic diameter of all tunnels. Thus the first upstream duct removes any entrance effect before the flow reaches the heated test section.

Air drawn through the duct and exhausted by blower which operates by a single- phase,  0.8 kW  electric  motor. A  photograph  of  the experimental apparatus is shown in Fig. (3).
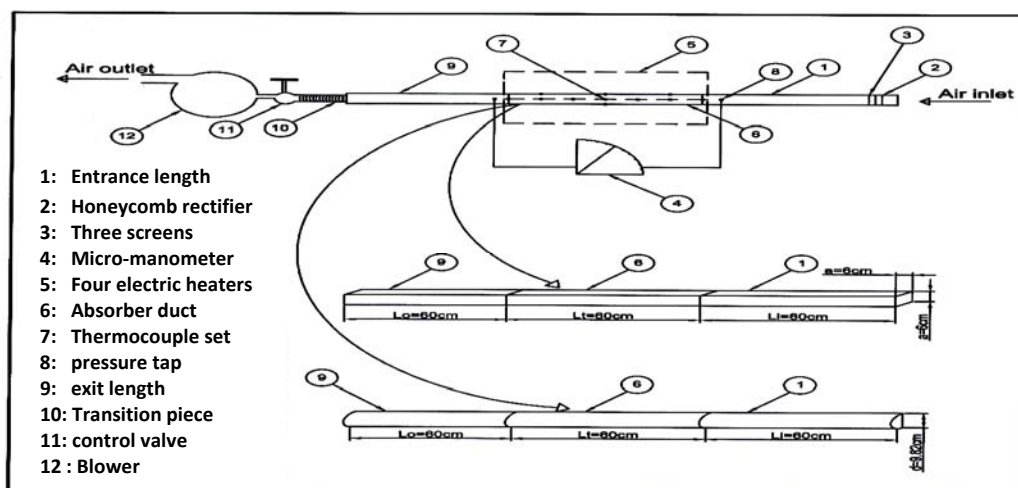


1: Entrance length
2: Honeycomb rectifier
3: Three screens
4: Micro-manometer
5: Four electric heaters
6: Absorber duct
7: Thermocouple set
8: pressure tap
9: exit length
10: Transition piece
11: control valve
12 : Blower

**Figure (2) : The schematic layout of the experimental apparatus**



**Figure (3) : A photograph of the experimental apparatus.**

For each shape of the cross-section geometry, three types of duct wall surface profile will be investigated. These types are; duct made from flat plate, duct made from sine-wave plate

and duct made from dimpled plate. A schematic diagram of geometry of the duct walls is given in Figure (4) while the main dimensions of the ducts

are presented in Table (1). A total of six ducts

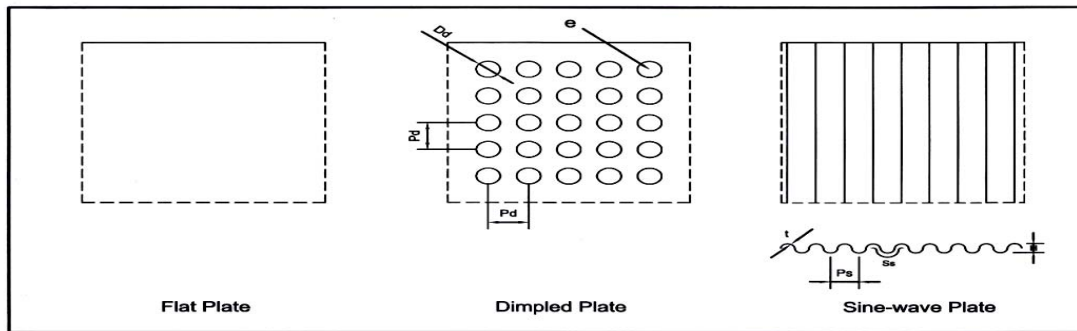sample will be tested as shown in Figure (5).



**Figure (4): Surface profiles of the ducts wall**

**Table (1): Main dimensions of the ducts**

| Material of duct | | (CuZn37) | |
| --- | --- | --- | --- |
| Duct thickness | | 0.5 mm | |
| Hydraulic diameter of ducts, ($d_h$) | | 6 cm | |
| Test section length, (Lt) | | 60 cm | |
| Semi-circular duct diameter, (d) | | 9.82 cm | |
| Side length of square duct,(a) | | 6 cm | |
| **Dimpled duct** | | **Sine-wave duct** | |
| Dimpled pitch length, (Pd) | 11 mm | pitch length, (Ps) | 8.5 mm |
| Dimpled diameter, (Dd) | 5.5 mm | Wave length, (Ss) | 10 mm |
| Dimpled depth, (e) | 2.3 mm | Amplitude, (H) | 2.5 mm |
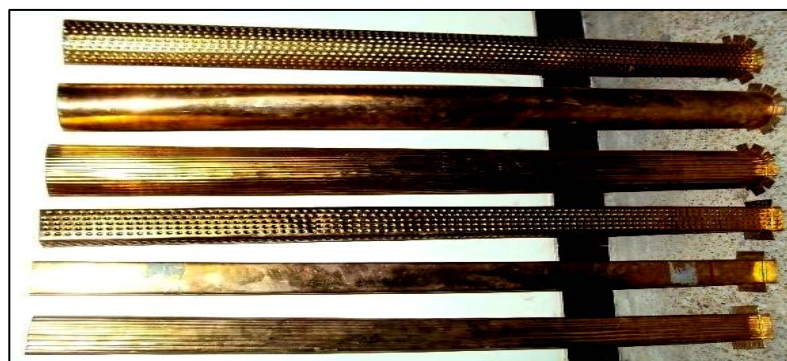


**Figure (5): Types of ducts used in this work**

The sinusoidally shaped duct walls were manufactured locally by bending. **Stasiek et al.** [1996] found that the most average value of pitch to amplitude ratio of wavy wall should be between (3) to (3.5) ,where this value gave a high heat transfer with lower pressure drop . Therefore, this ratio is kept constant at (3.4) throughout this work. The wire inserts (WI) are simple to manufacture and can be inserted inside these ducts to have a wide range of porosity. Also, it could be structured such that high thermal performance is maintained

while fluid pressure drop is held at reasonable levels. Hence, the WI can be configured to have a wide ranging of porosity and a large specific surface area. Different voids and diameter of wires can be introduced, so that thermal properties can be tuned to a special application.

In this work, The wired inserts used for experiments were manufactured by cutting commercial copper wires that provided from the local market with a diameter ($D_1$=1.7mm) and a length($L_1$=15m). These pieces were soldered

together to form the main frame for the WI as shown in Fig. (6-a). The spaces between the main frame were filled by using copper wire, with a

diameter of ($D_2$=0.5 mm) and a length of ($L_2$=140 m) as shown in the Fig. (6-b).
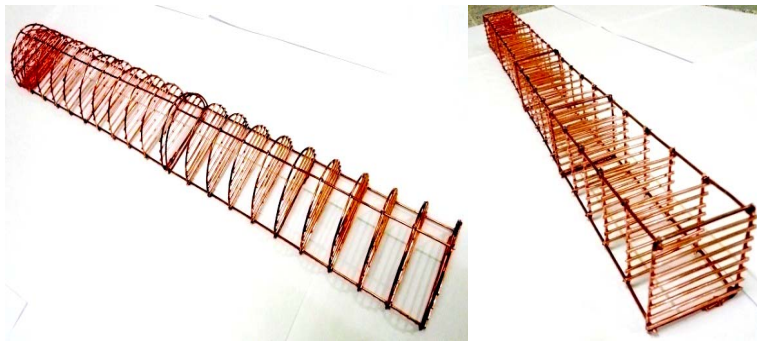
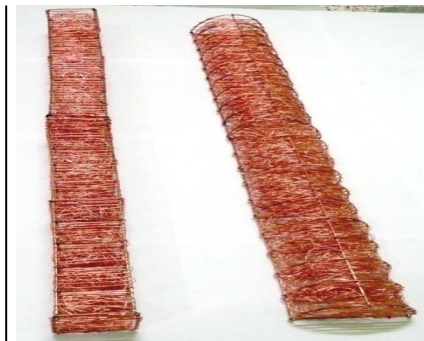- a -                                               - b -



**Figure (6): The square and semi-circular wired inserts**

The WI samples fit hardly in the ducts test section to force the air to flow through the WI and allowing only a negligible flow between the WI and the duct walls. So, each wired inserts is inserted into the test section axially slowly, so the strip doesn't scratch the inner wall of the duct and get deformed .According to **ASTM C127** [2004], the porosity of the wired inserts have been found to be 0.92 for both square and semi-circular wired inserts.

For indoor testing, the collector duct is heated by a four flexible radiant electric heaters. These heaters produce uniform heat flux along the test section. Each heater provides 1000 watts maximum and placed in a semi-circular shield made of aluminum plate. The structures of heaters have been installed on the adjustable slots to allow freedom of movement of the heater and trends for the situation that gives the required temperature degrees for the duct surface as shown in Fig (7).



**Figure (7): The Four heaters used in this work**

Each one of the heaters was connected to a Solid State Relay (SSR) to adjust the magnitude of the heat flux. During the experiments, the angle and the distance between heaters and the heat transfer test section has been changed for imposing axially and circumferentially constant wall temperature boundary condition.

Thermocouples type K were used to measure the temperature. The thermocouples were calibrated within ±0.2°C deviation before being used .Four thermocouples were fixed on the sides of the duct surface to measure the temperature of the duct surface as shown in Fig.(8)
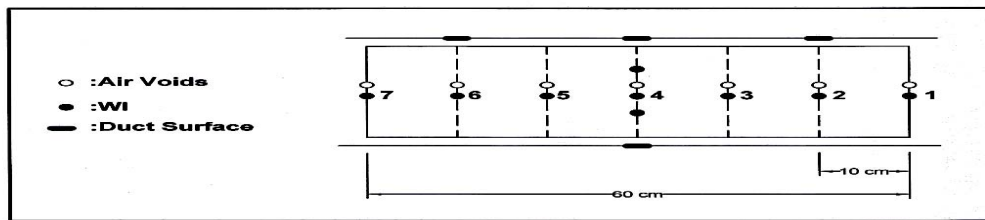
**Figure (8): Positions of the thermocouples on the heated section.**

The thermocouples were installed in an equally spaced distance to measure the temperatures at seven axial locations along the flow direction in the heater test section .Seven thermocouples instrumented in an equally spaced distance along the center line of the heated duct in the air voids between the WI; another seven thermocouple leads measured the WI temperatures. These thermocouples were glued directly on the WI surface. In addition, thermocouples are located in the WI surface at one-half the distance from the center line to the duct wall at x/L =0.5 .Another three thermocouples were used to measure the duct surface temperature profile at 1/6, 1/2 and 5/6of the test section length.

The pressure drop ($\Delta p$) across the wired inserts test section was measured by using adjustable slope micro-manometer. The friction factor was determined from pressure drop measurements in cold condition i.e. without heating the test section. This micro-manometer containing 0.784 specific gravity red fluid as a manometric liquid. This value of specific gravity ensures reasonable accurate measurement of the low pressure drop encountered at low Reynolds numbers.

The air velocities were measured by digital vane-type anemometer in different locations of the cross section .Five velocity reading were taken and the average of five reading was represented the velocity for each flow rate. A complete series of experiments consist of five Reynolds numbers ranging from the lowest possible flow at Reynolds number of 1825 to the largest possible flow at a Reynolds number of 7300 have been done.

All temperature measurements were taken at series of heated section types and Reynolds numbers. Before the measurements of each experimental run, the test rig was pressurized and any detected leak was carefully sealed .After the sources of leakage were treated from the ducting unit and heated test section, the test rig is ready for experimental runs. Tests were carried out for all the manufactured ducts with WI in the same rig. A constant heat input was supplied and the mass flow rate was adjusted so that the initial value of the Reynolds number was around 1825 .The temperatures of the air flow ,WI and duct surface along the heated section ,the mass flow rate of air as well as the pressure drop were continuously recorded .After collecting a set of data ,the mass flow rate of air was increased progressively until a maximum value of Re $_{WI}$ ~7300 was reaches .This procedure was repeated for all six ducts under investigation.

For each duct type, all experiments were performed at least twice (on different days), to check the repeatability of the data, which was proved to be good. Because the data demonstrated repeatability, only results from one of the tests will be presented here. The uncertainties for important parameters and measurements made during the current research have been carried out on the basis of the method proposed by **Kline and McClintock** [1953]. The maximum uncertainties are ±2.27% for

Dr. Mohammed H. Mahmoud
Dr. Fouad A. Saleh
Abeer H. Faleh

Compound Heat Transfer Enhancement in Dimpled
and Sinusoidal Metal Solar Wall Ducts Fitted with
Wired Inserts

Reynolds number, ±4.15% for Nusselt number and ±3.88% for friction factor.

## 4. Validity Test of Plain Duct

Prior to main experiments, the validity of the experimental set up was verified by conducting experiments for smooth duct. The convective heat transfer coefficient, h, was found by using the following equations;

$$Q° = m^o .C.( Ta_{out} - Ta_{in}) \tag{9}$$

$$Q° = h. A_C . ( LMTD) \tag{10}$$

$$LMTD = [(T_D - Ta_{in}) - (T_D - Ta_{out})] / Ln [(T_D - Ta_{in}) / (T_D - Ta_{out})] \tag{11}$$

Hence, the values for Nusselt number were computed from;   $Nu = h . d_h / k_a$   (12)

The experimental data were then compared with the results given by well known correlations under similar conditions. Figure(9,a and b) shows the comparison of the experimental values of Nusselt number and friction factor with those predicted by correlations proposed by **Gnielinski** [1976] for Nusselt number and by **Bhatti and Shah** [1987] for friction factor ;

$$Nu = 0.0214 (Re^{0.8} - 100)\{1 + (d_h/L)^{0.66}\} (T_b / T_D)^{0.45} Pr^{0.4} \quad \text{For } 2300 < Re < 10^6 \tag{13}$$

$$f = (1.0875 - 0.1125 \ H/W) \ fc \tag{14} \quad \text{, where fc = friction factor for the circular duct.}$$

$$= 0.0054 + 2.3*10^{-8} \ Re^{1.5} \qquad \text{for } 2300 < Re < 4000 \tag{15}$$

$$= 1.28*10^{-3} + 0.1143 \ Re^{-0.311} \qquad \text{for } 4000 < Re < 10^7 \tag{16}$$



(a)                                                          (b)
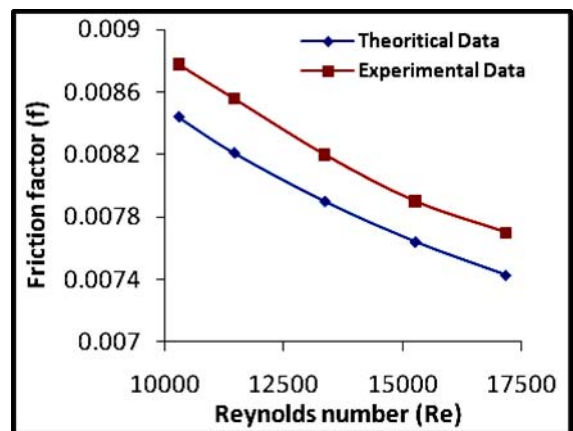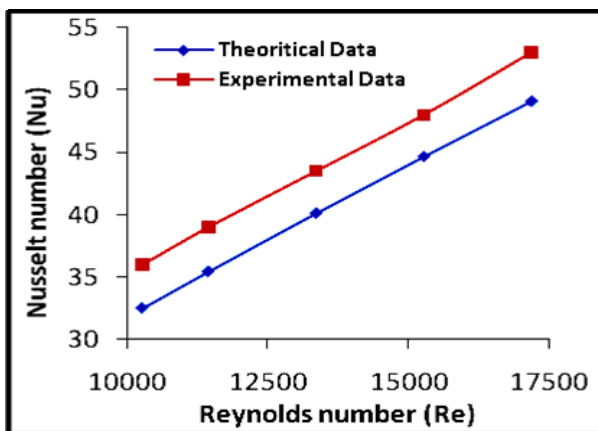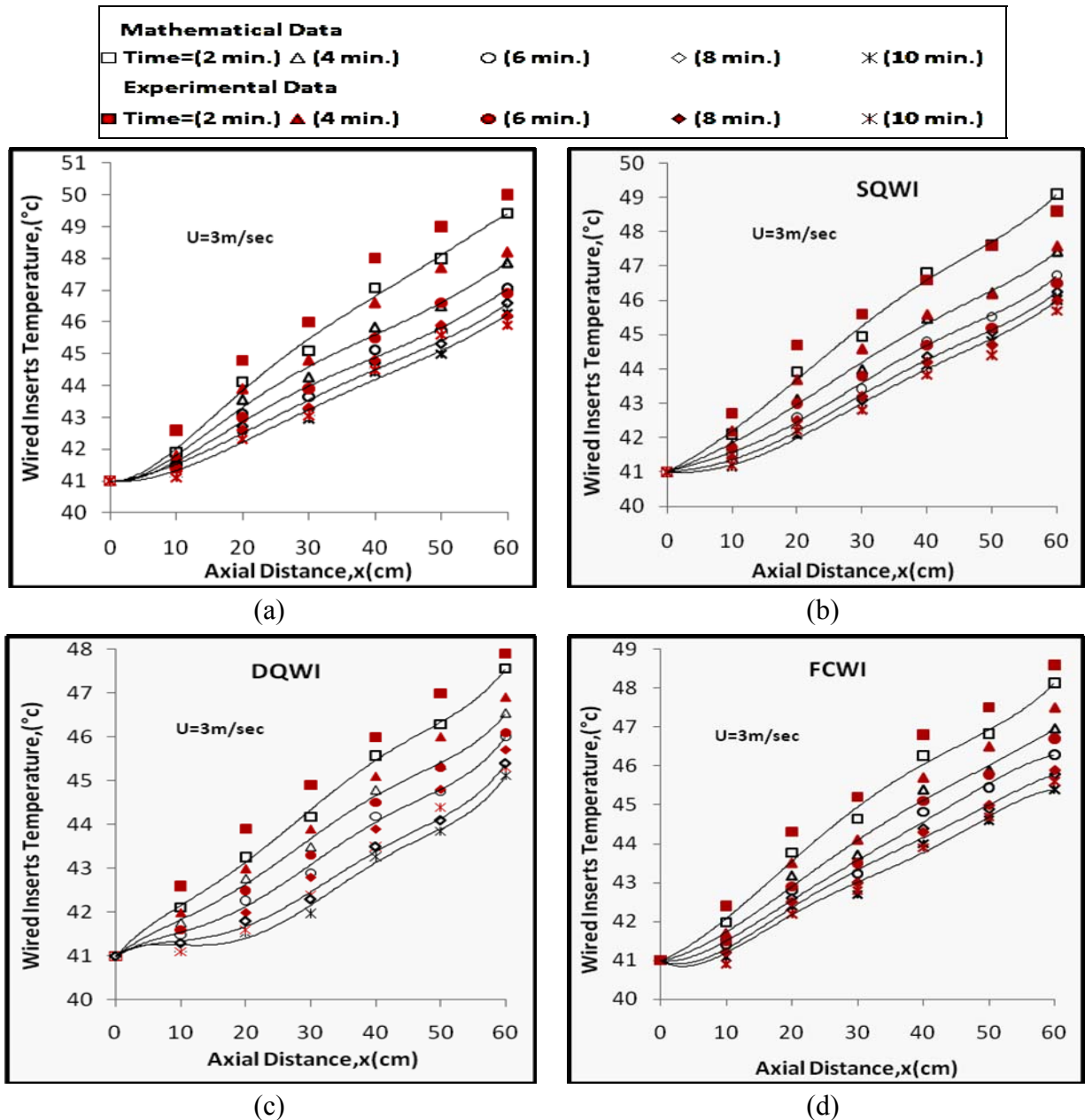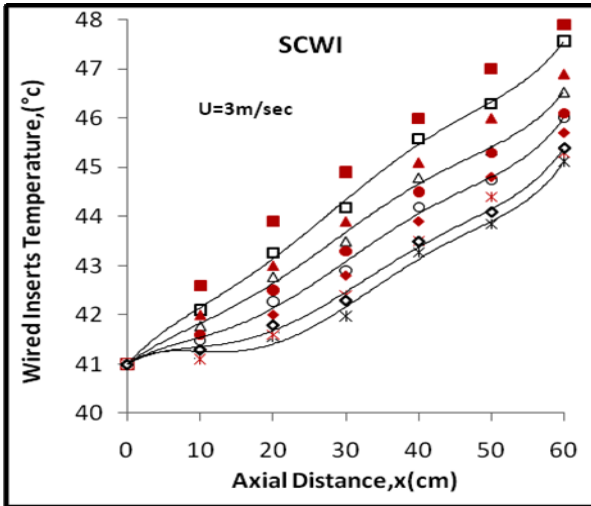
**Figure(9):Variation of Nusselt number and friction factor for square duct**

The present plain duct data is found to be in good agreement with previous correlations from the open literature. The experimental values of Nusselt number have a maximum deviation of 9.86%, whereas the friction factor has a maximum deviation of 5.13%. This ensures the accuracy of the experimental data obtained from the present experimental setup.
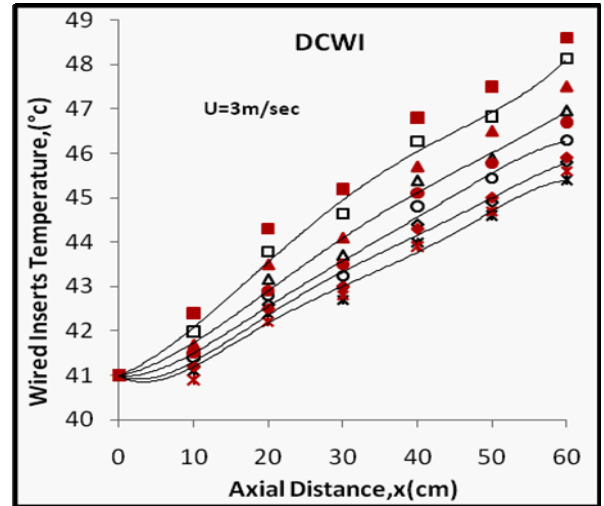
The results of the numerical computations were verified by the experimental tests. The exact conditions of the experiments performed were used in the numerical simulations, so that direct comparisons could be made. Typical results are shown in Figures (10) and (11) for the six different ducts under investigation.
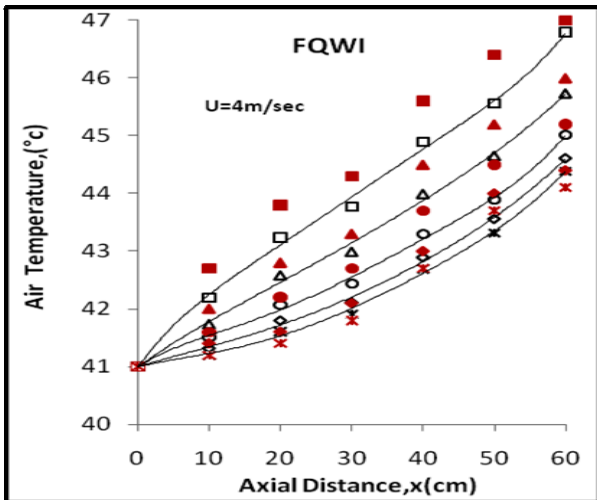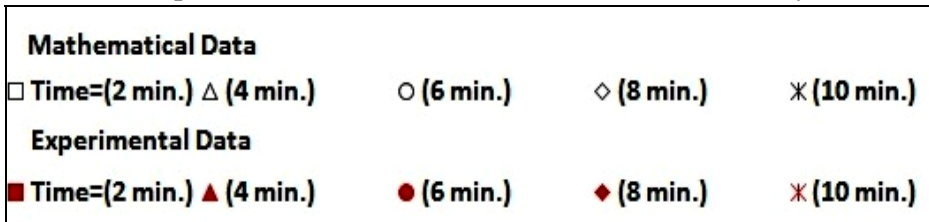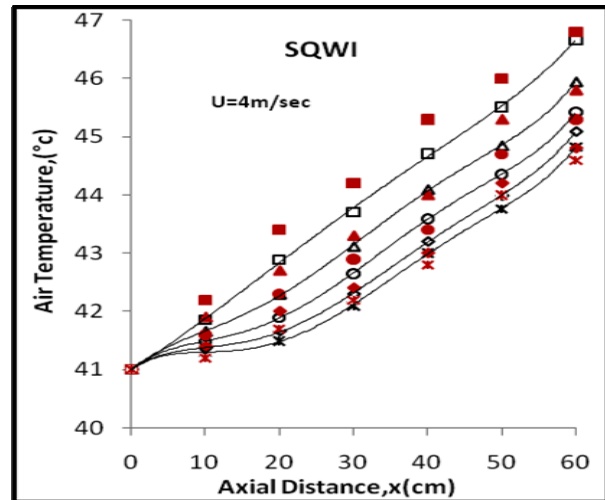
## 5. Results



(a)

(b)

(c)

(d)

Dr. Mohammed H. Mahmoud
Dr. Fouad A. Saleh
Abeer H. Faleh

Compound Heat Transfer Enhancement in Dimpled
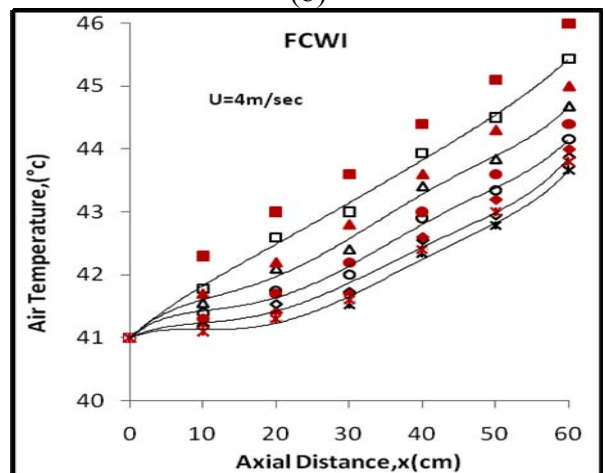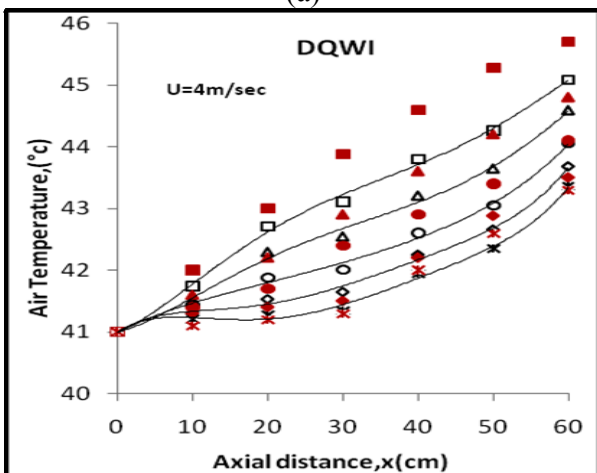and Sinusoidal Metal Solar Wall Ducts Fitted with
Wired Inserts

(e)



(f)

**Figure (10): Comparison between experimental and numerical
temperature distribution for WI at 3 m/sec air velocity.**





(a)



(b)



(c)

(c)                                    (d)



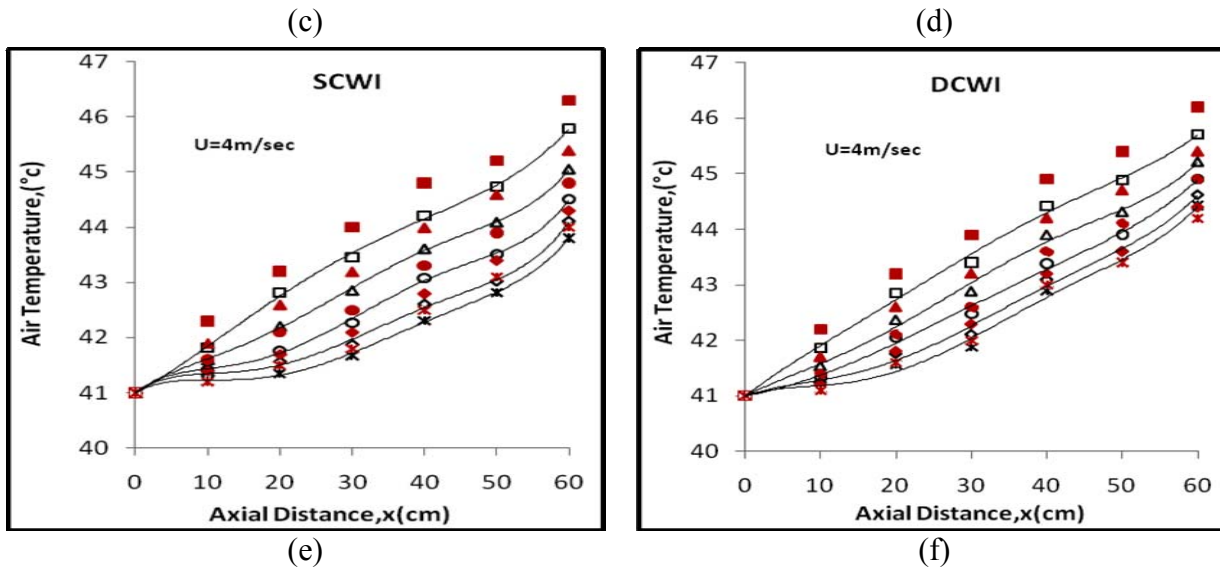(e)                                    (f)

**Figure (11): Comparison between experimental and numerical temperature distribution for air at 4 m/sec air velocity.**

The temperature profiles of both experiments and numerical simulations show that the results obtained from both these measurement techniques are in same general trends. In general, the agreements between mathematical and experimental results demonstrate that the computational scheme is adequately accurate to predict the transient thermal response of the MSW. It is clear from these figs. that both the air and WI (mathematical and experimental) temperature increases with the axial distance (x) of the test section but decreases with time of heating. Generally, the rate of increase in temperature is higher at the beginning than at the end of heating period because of the higher temperature difference existing at the beginning. The different response for each type of six ducts is clear in these Figures. The temperature fields of gases decrease in the direction of air flow through the heated section more rapidly for DQWI than FCWI and even FQWI.

Figure (12) shows the variation of the mathematical and experimental WI and air temperatures as a function of time at dimensionless distance (X/L=0.5) at the center point of the heated test section for various $Re_{WI}$. It

is clear from these figs. that the temperature of air and WI (mathematical and experimental) decreases with time and decreases when the Reynolds number increase .This is an expected feature, as the air flow velocity is increased, the residence time is decreased, therefore, the exposure to heat transfer is decreased .With decreased exposure to the hot surface, the air will have a lower resulting temperature. The wired inserts temperature is higher than the air temperature at the same point because the WI specific heat capacity is higher than air .The theoretical result deviate from experimental data at the beginning of the heating period  and then continuously decreased with progress of time.

Figure (13, a and b) shows the variation of outlet WI and air temperatures with $Re_{WI}$ at time (t=10 min.)**.** When the velocity is increased, an inefficient use of the unit for energy transfer has been determined, indicating the very important effect of the velocity. It is observed that modifying duct surface profile and duct cross-section geometry yields, appreciable temperature rise in the exit air. It's clear from these figures that the temperatures values for both the WI and air of flat, square duct with wired inserts are higher than the

603

other ducts. Therefore, by selecting the optimum type of ducting geometry and surface profile for the MSW, it is possible to increase the air outlet temperature with storing the excess energy in the WI at the same time.

The comparisons between experimental and numerical results in all above figures show that the predications produced by the present numerical model are reasonable for all ducts under investigation. However, it may be noted that there is a little difference between experimental and numerical data ( the maximum difference is ± 5.72% ) . This difference is believed to be mainly due to the effect of selected Nusselt number equations, as there is no such suitable equation available for each one of the ducts under investigation. Since the transient method can spend less time and money and give a more accurate measurement than the conventional steady-state method does, it is worth employing the transient method to measure the heat transfer coefficient in porous channels ( **Jeng et al.** [2004] ).
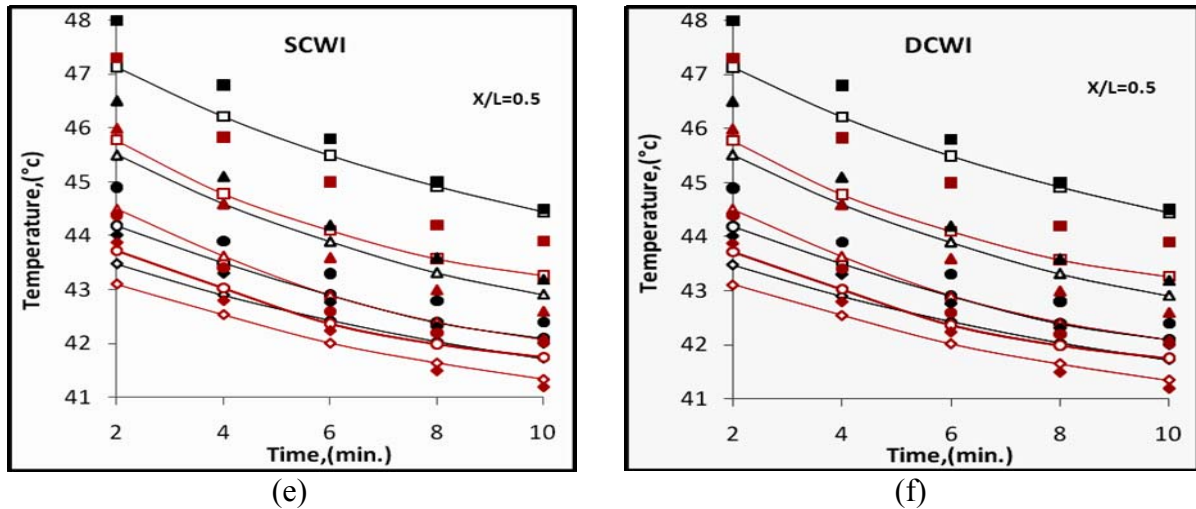


(a)

(b)

(c)

(d)

(e)                                                              (f)
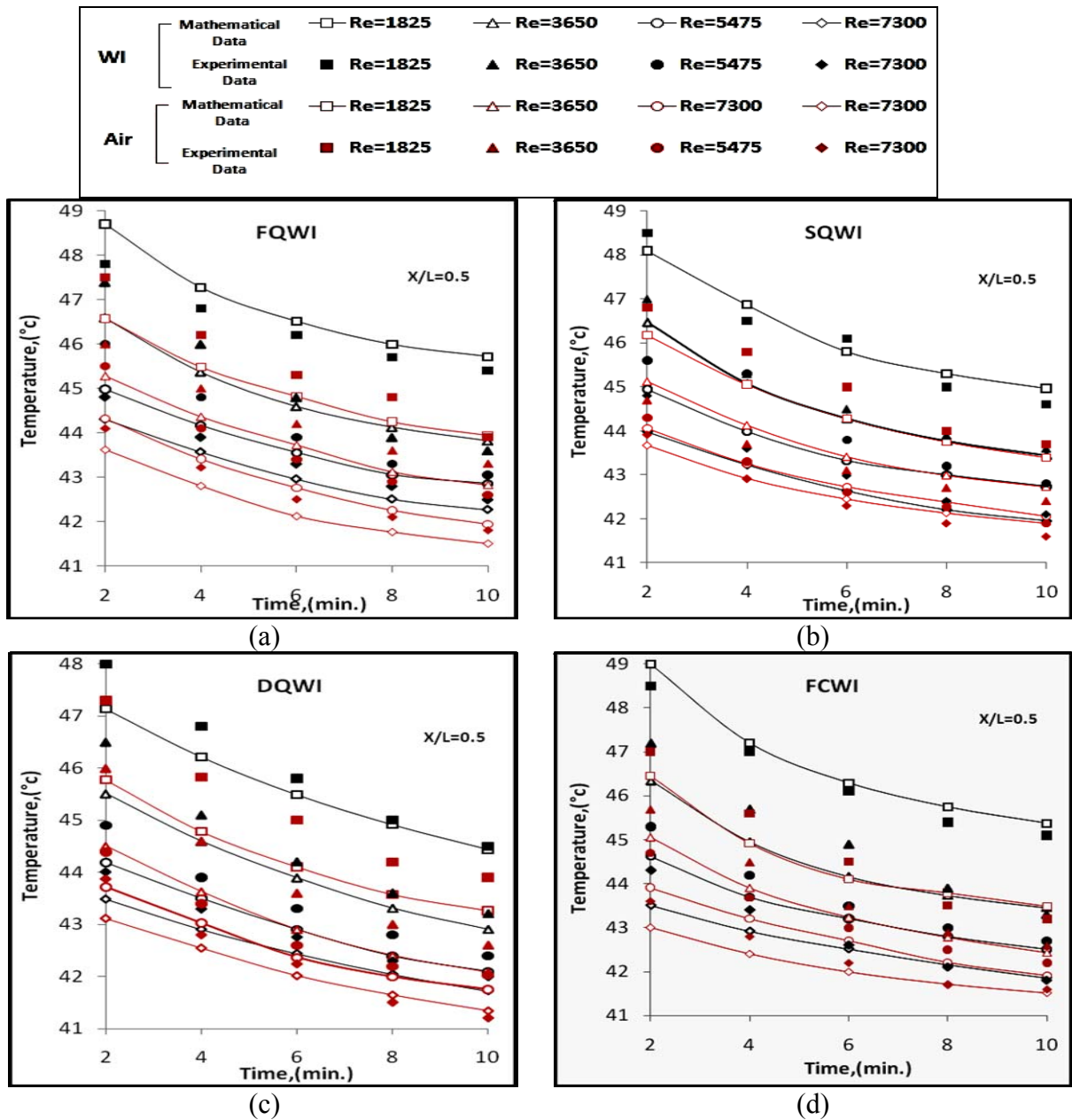
**Figure (12): Variation of WI and air temperature distribution with time
at different Reynolds number.**



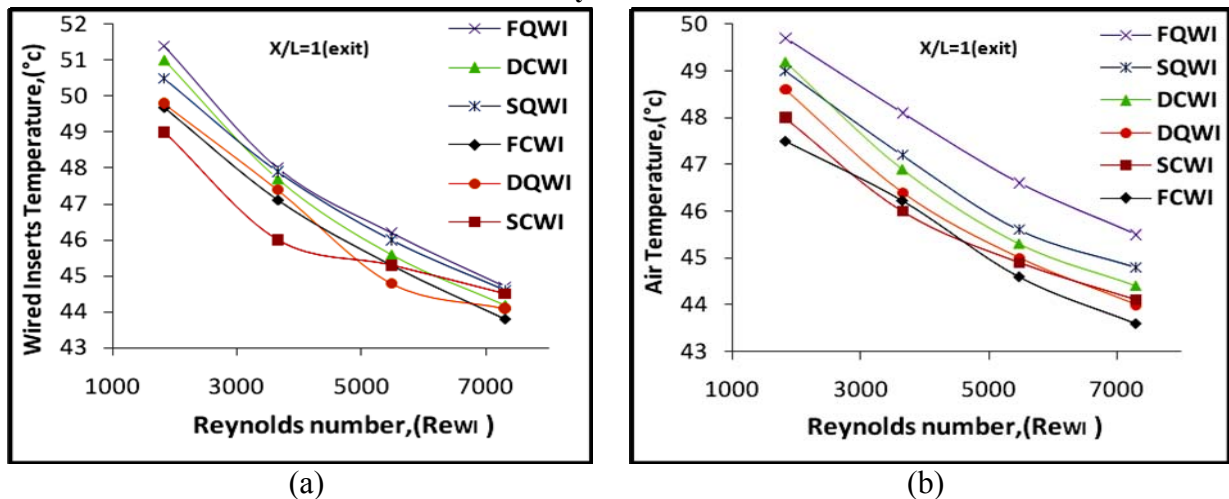(a)                                                              (b)

**Figure (13):Variation of outlet temperatures with Re$_{WI}$ at time (t=10 min.).**

Therefore, a Nusselt number correlation equation has been developed for each type of the ducts by selecting the value of the Nusselt number that causes the result of the numerical model to fit best the experimental data at each Reynolds number. All the data necessary to run the computer program are known, except for the expression of the Nusselt number. This method for the calculating the Nusselt number was used by **Coutier and Farber** [1981] to develop a new empirical equation for the volumetric heat transfer coefficient ( $= h_*A_s$). Fig.(14) presents the Nusselt number for different types of ducts under investigation at various Reynolds numbers.
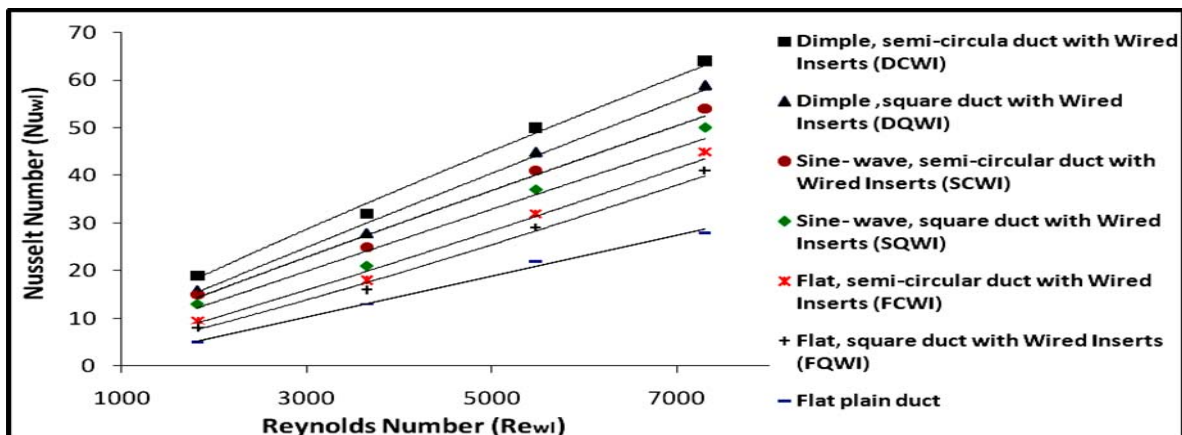


**Figure (14): Effect of the duct geometry and WI on the Nusselt number**

Dr. Mohammed H. Mahmoud
Dr. Fouad A. Saleh
Abeer H. Faleh

Compound Heat Transfer Enhancement in Dimpled
and Sinusoidal Metal Solar Wall Ducts Fitted with
Wired Inserts

The results show that the Nusselt number (and therefore, the heat transfer coefficient) increases with increasing Reynolds number depending on the wired inserts Reynolds number ($Re_{WI}$). It's clear from Figure (14) that the Nusselt number of the dimpled ducts with a wired inserts are higher than all other ducts. It seems that the dimples generate strong vortices, which produce higher turbulence around the dimples and in the down stream area of the dimples, thus enhancing the heat transfer. From this Fig. it is noted that the Nusselt number for semi-circular dimpled duct is higher than square dimpled duct. Results reveal

that the heat transfer rate from using both WI and dimpled or sinusoidal duct walls is higher than that from using WI alone. It is found that the Nusselt number in the DCWI is (44.2% -100%) greater than the values of the flat duct with WI. The results show that the improvement in Nusselt number for flat duct with WI is (1.4 - 2) times the values for flat duct with no WI.

The pressure drop importance is not only in selecting the fan but also in ensuring a uniform flow of air in the duct. Figures (15) and (16) show the influence of duct type on the friction factor and the pressure loss, respectively.
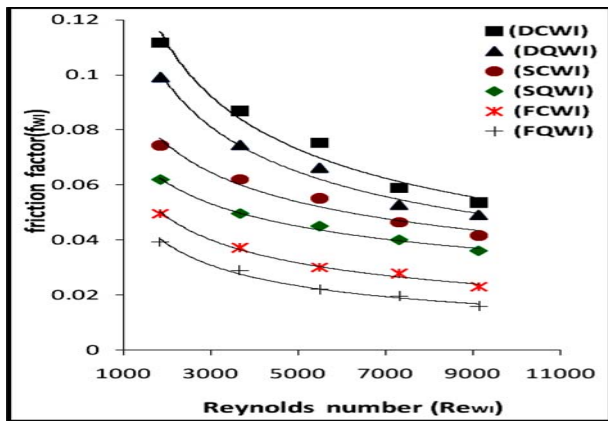


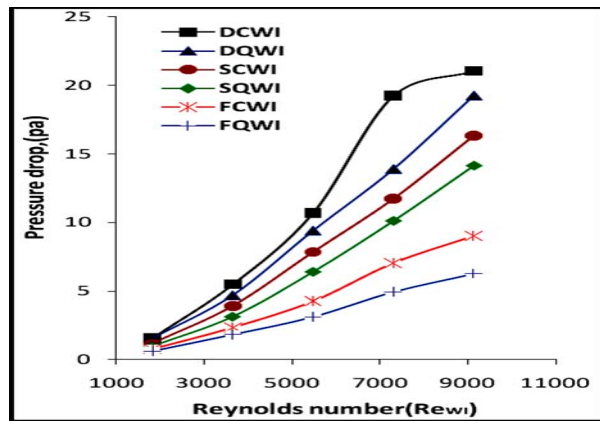**Figure (15): Variation of friction factor with Reynolds number.**



**Figure (16): Variation of pressure drop with Reynolds number**

The result show that the friction factor in the dimpled ducts combined with a WI are higher than other ducts because of the higher flow mixing effect for the dimpled duct that leading to greater turbulence intensity. It's shown from Figure (16) that the largest pressure drop occurs at duct yield the highest value of Nusselt number i.e. Dimpled, semi- circular duct with Wired Inserts DCWI. It is found that the pressure drop in the DCWI is (101.27% -127.8%) greater than the value of the duct with WI.

It would be useful for the practicing engineer if the results of Nusselt number and friction factor are presented as a function of the Reynolds number. By using the data predicted in Figures (14) and (15); six new correlations for Nusselt number and friction factor were developed to assess the real benefits in using the WI and the dimpled and sine – wave duct walls. The correlations are shown in Table (2).

**Table (2): Predicted $Nu_{WI}$ and $f_{WI}$ correlations at 1825< $Re_{WI}$<7300.**

| Duct Geometry | $Nu_{WI}$ correlation | $R^2$-value | $f_{WI}$ correlation | $R^2$-value |
|---|---|---|---|---|
| DCWI | $Nu_{WI}=0.026\ Re_{WI}^{0.871}$ | 0.9934 | $f_{WI}=3.659\ Re_{WI}^{-0.46}$ | 0.9711 |
| DQWI | $Nu_{WI}=0.012\ Re_{WI}^{0.95}$ | 0.9935 | $f_{WI}=2.766\ Re_{WI}^{-0.44}$ | 0.9816 |
| SCWI | $Nu_{WI}=0.013\ Re_{WI}^{0.933}$ | 0.9875 | $f_{WI}=1.112\ Re_{WI}^{-0.35}$ | 0.9651 |
| SQWI | $Nu_{WI}=0.007\ Re_{WI}^{0.983}$ | 0.9755 | $f_{WI}=0.729\ Re_{WI}^{-0.32}$ | 0.9901 |
| FCWI | $Nu_{WI}=0.002\ Re_{WI}^{1.112}$ | 0.9905 | $f_{WI}=1.586\ Re_{WI}^{-0.46}$ | 0.9863 |
| FQWI | $Nu_{WI}=0.001\ Re_{WI}^{1.188}$ | 0.9929 | $f_{WI}=2.464\ Re_{WI}^{-0.54}$ | 0.9868 |

As far as known, no study has determined the Nusselt number in duct filled across the entire cross-section with WI in conjunction with dimple-shape or sinusoidal-shape roughness geometry for the duct walls. Therefore, no comparison with other data can be provided.

One of the most important results for the purpose of this research is the compactness factor. The compactness factor is a ratio of the heat transfer to pressure drop. The definition of compactness factor is CF =j/f , where j is the Colburn factor and f is the friction factor. Figure (17) represents the thermo-hydraulic performance ratio as a function of the Reynolds number for all different ducts under investigation.
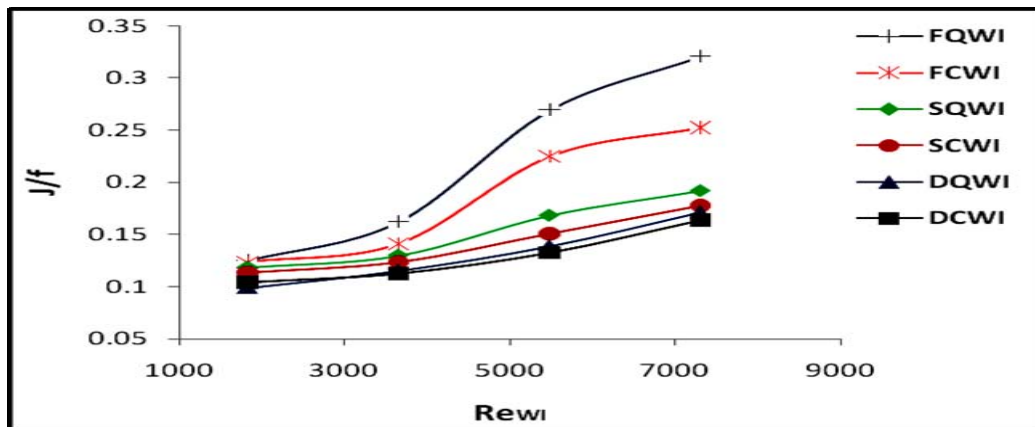


**Figure (17): Variation of compactness factor with Reynolds number**

It's clear from this figure that the [FQWI] shows the highest performance especially at high Reynolds numbers. Except for ducts with flat walls, all other types of ducts show very small dependence of compactness factor on the Reynolds number.

The enhancement efficiency of Roughened square and semi-circular duct walls ($\eta_e$) is defined as:

$$\eta e = \frac{Nu_R}{Nu_F} \qquad (17)$$

Figure (18) presents of $\eta_e$ as a function of the Reynolds number for sine-wave and dimpled wired inserts ducts. It's clear from this figure that the enhancement efficiency tends to decrease with the rise of Reynolds number but variation is not the same for each type of the ducts roughness. The enhancement efficiency for sine-wave duct walls is nearly uniform at Reynolds number above 6000 and tends to reduce to unity .This indicates that the sinusoidal shaped duct walls is not feasible in terms of energy saving at higher Reynolds number. The results reveal that DCWI provides enhancement efficiency values higher than all other types of ducts.
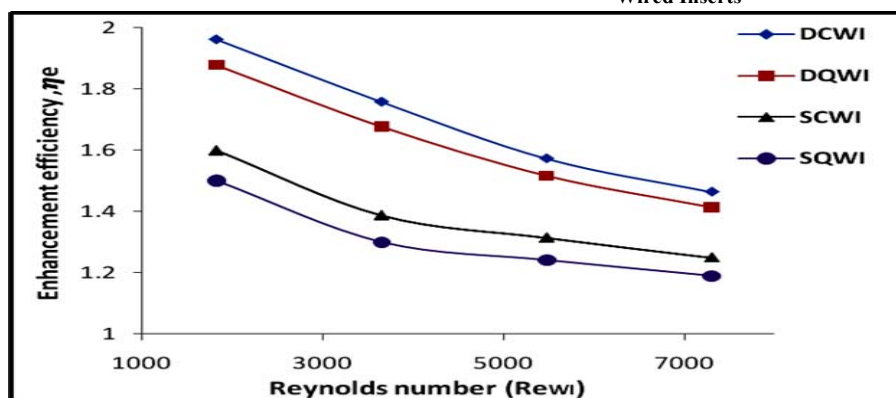
Dr. Mohammed H. Mahmoud
Dr. Fouad A. Saleh
Abeer H. Faleh

Compound Heat Transfer Enhancement in Dimpled
and Sinusoidal Metal Solar Wall Ducts Fitted with
Wired Inserts

**Figure (18): Variation of enhancement efficiency with Reynolds number**

## 6. Conclusions:

Within the limitations of materials and experimental results obtained in this work, the main conclusions may be summarized as follows**:**

1- The two-dimensional numerical approach is generally found to be agreeing reasonably with the experimented results obtained in this work ( the maximum deviation is found to be ± 5.72%). These agreements demonstrate that the computational scheme is adequately accurate to predict the transient behavior of the MSW ducts.

2- Six new correlation equations for the Nusselt number were devised for each type of ducts under investigation. The developed transient technique for determining the Nusselt number correlation was the best match between the measured experimental data and the one calculated by the numerical model. As far as known, no Nusselt number correlations in the open literatures for the same geometric design of the ducts under investigation.

3- It is found that the FQWI has the highest exit air temperature.

4- The results show that the Nusselt number for semi-circular duct is higher than that of square duct. The Nusselt number of DCWI was found to be (44.2% - 100%) greater than the values of flat duct with WI. The improvement in Nusselt number for flat duct with WI is found to be (1.4 – 2) times the value of flat duct with no WI.

5- The DCWI duct is found to be the most effective for heat transfer enhancement, but also to have the greatest pressure drop increase. The results show that the pressure drop in the DCWI is (101.27% - 172.8%) greater than the value of flat duct with WI.

6- Six design correlation equations for predicting the MSW ducts friction factors have been developed. It was found that the FQWI duct has the lowest friction factor.

7- The enhancement efficiency of the roughened walls tends to decrease with rise of Reynolds number, but the variation is not the same for each type of the ducts. It is found that the DCWI provides enhancement efficiency values higher than other types of ducts. Results indicate that the sinusoidal duct walls are not feasible in terms of energy saving at high Reynolds number.

8- The results of the compactness factor show different response. It is found that the FQWI has the highest performance especially at high Reynolds numbers. Except for ducts with flat walls, all other types of ducts show very small

dependence of compactness factor on the Reynolds number.

Although the present study was related to MSW ducts, the results were of more general interest for any investigation related to compound metallic inserts for enhancing heat transfer.

**References :**

* Aldabbagh a, L.B.Y. Egelioglu a,F. and Ilkan b,M., **"Single and Double Pass Solar Air Heaters with Wire Mesh as Packing Bed"** , Energy ,Vol.36, May 2011.

* Annual Book of ASTM Standards, Vol.04 02 , section E-11, 2004.

* Bhatti, M.S., R.K. Shah, **"Turbulent and Transitional Flow Convective Heat Transfer"**, Hand book of Single-phase Convection Heat Transfer, John Wiley, NY, 1987.

* Bilgen ,E., **"Conjugate Heat Transfer by Conduction and Natural Convection on a heated Vertical Walls"** ,Applied Thermal Engineering ,Vol.29, 2009.

* Chang,S.W., K.F. Chiang, T.C. Chou, **"Heat Transfer and Pressure Drop in Hexagonal Ducts with Surface Dimples"**, Exp. Thermal and Fluid Science, Vol. 34, 2010.

* Coutier, J.P. and E.A. Farber, **"Designing Rock Beds as Storage Units for Solar Air Systems Using an Optimized Method Based on Numerical Model"**, Proceeding of I.S.E.S. Congress, Brighton, England, Aug.1981.

* Dukhan, N. and Kuan-Chih Chen, **" Heat Transfer Measurements in Metal Foam Subjected to Constant Heat Flux"**, Exp. Thermal and Fluid Science, Vol. 32, 2007.

* Durmus ,A., H.Benli , I.Kurtbas and H.Gul , **"Investigation of Heat Transfer and Pressure Drop in plate Heat Exchangers Having Different Surface Profiles "** , Int. J. of Heat and Mass Transfer ,Vol.52, 2009.

* Gnielinski,**V., "New Equation for Heat and Mass Transfer in Turbulent Heat Channel Flow"**, Int. J. Chem. Eng., Vol.16(2), 1976.

* Jeng, T.M., M.P. Wang, G.J. Hwang and Y.H. Hung, **"A New Semi-empirical Model for Predicting Heat Transfer Characteristics in Porous Channels"**, Experimental Thermal and Fluid Science, Vol.29, 2004.

* Kline, S. J. and F.A. McClintock, **"Describing uncertainties in single sample experiments"**, Mech. Eng., Vol. 75, 1953.

* Mengna, H., D. Xianhe, H. Kuo and L. Zhiwu, **"Compound Heat Transfer Enhancement of a Converging–diverging Tube with Evenly Spaced Twisted-tapes"**, Chinese Journal of Chemical Eng., Vol.15, 2007.

* Piao,Y, E.G .Hauptmann, and M.Iqbal, **"Forced Convection Heat Transfer in cross-corrugated Solar Air Heaters"**, J. of Solar Energy Eng., Tr. of ASME , Vol. 116, 1994.

* Pramanik, D. and S. K. Saha, **"Thermo-hydraulics of Laminar Flow Through Rectangular and Square Ducts with Transverse Ribs and Twisted Tapes"**, J. of Heat Transfer, Tr. of ASME, Vol. 128, 2006.

* Prasad, S.B., J.S. Saini, Krishna M. Singh, **"Characteristics of Packed Bed Solar Air Heater Using Wire Mesh Investigation of Heat Transfer and Friction as Packing Material"**, Solar Energy, Vol. 83, 2009.

* Promvonge, P., and S. Eiamsa, **"Heat Transfer Behaviors in a Tube with**

Dr. Mohammed H. Mahmoud
Dr. Fouad A. Saleh
Abeer H. Faleh

Compound Heat Transfer Enhancement in Dimpled
and Sinusoidal Metal Solar Wall Ducts Fitted with
Wired Inserts

**Combined Conical-ring and Twisted-tape Insert"**, Int.Com. in Heat and Mass Tr.,Vol.34, 2007.

* Saini, R.P. and J. Verma, **"Heat Transfer and Friction Factor Correlations for a Duct Having Dimple-Shape Artificial Roughness for Solar Air Heaters"**, Energy, Vol. 33, 2008.

* Sang Dong Hwang, Hyun Goo Kwon and Hyung Hee Cho, **"Heat Transfer with Dimple/Protrusion Arrays in a Rectangular Duct with a Low Reynolds number range"**, Int. J. of Heat and Fluid Flow, Vol. 29, 2008.

* Stasiek,J.,M.collins, M.Ciofalo,and P.Chew ,**"Investigation of Flow and Heat Transfer in Corrugated Passages"** , Int. J. Heat Mass Transfer, Vol.39, 1996.

* Thianpong, C., P. Eiamsa, K. Wongcharee and S. Eiamsa, **"Compound Heat Transfer Enhancement of a Dimpled Tube with a Twisted Tape Swirl Generator"**, Int. Com. in Heat and Mass Transfer, Vol. 36, 2009.

## Nomenclatures:

| | | | | |
|---|---|---|---|---|
| A | : Cross–sectional area of the duct, $(m^2)$ | | L | : Length , (m) |
| As | : Surface area per unit volume, (1/m) | | $\overset{o}{m}$ | :Mass flow rate , (kg/s) |
| C | : Specific heat, (J/kg.K) | | Nu | :Nusselt number |
| CF | **:** Compactness Factor | | p | : Pressure, (kPa) |
| $d_h$ | **:** Hydraulic diameter of ducts, (m) | | Pr | : Prandtle number |
| $D_h$ | : Hydraulic diameter of Wired Inserts, (m) | | $\dot{Q}$ | : Rate of heat transfer , (W) |
| f | **:** Friction factor | | Re | : Reynolds number |
| h | : Area heat transfer coefficient, $(W/m^2.K)$ | | t | **:** Time , (s) |
| H/W | : Height to width ratio | | T | **:** Temperature $(^oC)$ |
| J | **:** Colburn factor = $St.Pr^{2/3}$ | | u | **:** Flow velocity, (m/s) |
| K | **:** Thermal conductivity, (W/m. K) | | x | : Axial distance ,(m) |

## Subscripts:

| | |
|---|---|
| a | : air |
| b | : bulk |
| c | : contact |
| D | :duct wall |
| F | : flat wall |
| o | : outside |
| R | : roughened |
| SD | : surface area |

## Abbreviations:

| | |
|---|---|
| ASTM | : American Society for Testing and Materials |
| DCWI | :Dimpled, semi-circular duct with Wired Inserts |
| DQWI | : Dimpled, square duct with Wired Inserts |
| FCWI | : Flat, semi-circular duct with Wired Inserts |
| FQWI | : Flat, square duct with Wired Inserts |
| LMTD | : Log. Mean Temperature Difference |
| MSW | : Metal Solar Wall |
| SCWI | : Sine-wave, semi-circular duct with Wired Insert |
| SQWI | : Sine -wave, square duct with Wired Inserts |

## Greek Letters:

| | |
|---|---|
| ε | :Void fraction |
| ρ | : Density |
| $\eta_e$ | : efficiency |